Clinical and Translational Radiation Oncology 33 (2022) 37–44

Contents lists available at ScienceDirect

Clinical and Translational Radiation Oncology

journal homepage: www.sciencedirect.com/journal/clinical-and-translational-radiation-oncology

Original Research Article

Extraction parameter optimized radiomics for neoadjuvant chemotherapy response prognosis in advanced nasopharyngeal carcinoma

Yiling Wang [a,*], Churong Li [a], Gang Yin [a,*], Jie Wang [a], Jie Li [a], Pei Wang [a], Jie Bian [b]

[a] Sichuan Cancer Hospital & Institute, School of Medicine, University of Electronic Science and Technology of China, Radiation Oncology Key Laboratory Of Sichuan Province, Chengdu, China
[b] First People's Hospital of Liangshan, Sichuan, China

ARTICLE INFO

Keywords:
Nasopharyngeal carcinoma
Neoadjuvant Chemotherapy prognosis
Radiomics

ABSTRACT

Background and purpose: Neoadjuvant Chemotherapy (NAC) followed by concurrent chemoradiotherapy (CCRT) is promising in improving the survival rate for advanced nasopharyngeal carcinoma (NPC) patients relative to CCRT alone. However, not all patients respond well to NAC. Therefore, we aimed to develop and evaluate a modified radiomics model for the NAC response prognosis in NPC patients.

Methods: A total of 165 patients with biopsy-proven locally advanced NPC were retrospectively selected from the database of our hospital. 85 out of them were for training and cross-validation, while the other 80 patients were for independent testing. All patients were treated with NAC and underwent MRI inspection, including T1-weighted (T1), T2-weighted (T2), and contrast-enhanced T1-weighted (T1-cs) sequences before and after two cycles of NAC. We classified the patients into the response or non-response groups by the Response Evaluation Criteria in Solid Tumors 1.1 (RECIST 1.1). Radiomics features were extracted from the primary and lymph node gross tumor volume in each sequence. To further improve the predictive performance, the permutation of multiple combinations of extraction parameters has first ever been investigated in the NAC prognosis for NPC patients. The model was constructed by logistic regression and cross-validated by bootstrapping with a resampling number of 1000. Independent testing was also implemented. In addition, we also applied an imbalance-adjusted bootstrap strategy to decrease the bias of small samples.

Results: For the cross-validation cohort, the resultant AUC, sensitivity, and specificity in terms of 95% confidence interval were 0.948 ± 0.004, 0.849 ± 0.005, and 0.840 ± 0.010. For the independent testing cohort, the model reached an AUC of 0.925, a sensitivity of 0.821, and a specificity of 0.792. There was a significant difference in the estimated radiomics score between the response and non-response groups ($P < 0.005$).

Conclusions: An MRI-based radiomics model was developed and demonstrated promising capability for the individual prediction of NAC response in NPC patients. In particular, we have optimized the multiple combinations of texture extraction parameters with the permutation test and observed an encouraging improvement of the prediction performance compared to the previously published studies. The proposed model might provide chances for individualized treatment in NPC patients while retrenching the cost of clinical resources.

Introduction

Nasopharyngeal carcinoma (NPC) is one of the prevailing rare malignancies in Southeast Asia, with an annual incidence of up to 500 cases per million individuals for the endemic high-risk areas [1], and the global mortality of NPC could be 72,987 individuals per year [2]. In clinical practice, radiotherapy (RT), especially intensity-modulated RT, is the most common treatment for NPC due to the intrinsic high radiosensitivity of the nasopharynx [3]. Besides, as have been demonstrated by abundant studies, the survival rate of NPC patients could be further prolonged by combining RT with chemotherapy, such as the extensively applied concurrent chemo-radiotherapy (CCRT), adjuvant chemotherapy (AC), and neoadjuvant chemotherapy (NAC) [4–8]. Specifically, NAC is implemented before standard CCRT or RT, which is a promising alternative for locally advanced NPC with potentially decreased distant failure, and increased overall survival rate [9,10].

However, in clinical practice, not all NPC patients respond

* Corresponding authors.
E-mail addresses: mara.wangyiling@gmail.com (Y. Wang), cxqyguestc@163.com (G. Yin).

https://doi.org/10.1016/j.ctro.2021.12.005
Received 6 July 2021; Received in revised form 6 November 2021; Accepted 19 December 2021
Available online 29 December 2021

effectively to NAC, and individual differences could exist in tumor control rate and progression [11,12], which could play a significant prognostic influence on the disease-free and overall survival rates [13]. Therefore, predicting the response of NAC for NPC patients may play a considerably important role in avoiding the unnecessary side effect of NAC, paving the way towards precision and individualized therapy, and benefiting the quality of life for NPC patients.

To date, many studies have demonstrated the potential capability of multi-modality magnetic resonance imaging (MRI) in characterization and prognosis assessment [14,15]. While in recent years, it is advanced for quantitative imaging analysis via an emerging technology, radiomics [16–18]. Acted as imaging biomarkers, it could characterize the tumor heterogeneity and histological changes, therefore decoding the hidden traits to the genetic and molecular levels and benefiting the treatment decision [30]. For NPC, while previous studies have investigated the potential prognostic ability of radiomics in terms of local and distant failure [19], classification of distinct survival groups [20], local recurrence [21], and CCRT treatment response [22], limited efforts have been made for the NAC response prediction [23,37]. With an area under the receiver operating characteristic curve values (AUC) [27] to be 0.82–0.86, the published result demonstrated a promising capability of NAC prognosis prediction in NPC patients. However, there still exists a promotion space for predictive performance. Besides, independent testing should also be complemented to evaluate the prediction performance more comprehensively. Furthermore, to provide therapeutic guidance in the clinic, there is still an urgent demand to develop a more accurate predictive model for NAC response in NPC patients.

This study aims to improve the effectiveness of MRI radiomics for pretreatment prediction of the response to NAC in patients with locally advanced NPC. The permutation and combination of multiple texture extraction parameters, which were demonstrated to be effective for soft-tissue sarcomas prognosis [24], has first ever been investigated in the NAC response prognosis for NPC patients. Besides, to further validate the predictive performance, independent testing is implemented. The imbalance-adjusted bootstrap strategy is also applied to decrease the defect of small samples.

Methods and materials

Patients

We collected data from Sichuan Cancer Hospital & Institute. Informed consent has been obtained from all patients, and anonymization was implemented subsequently with in-house codes. A total of 200 patients with biopsy-proven locally advanced NPC (stage III–IVb) treated by platinum-based NAC before radiotherapy were enrolled in this study (100 between January 2009 to December 2014, 100 between June 2016 to February 2018). Based on the inclusion and exclusion criteria where samples with lesion diameter smaller than 5 mm, inadequate NAC (at least two cycles), treatment elsewhere, or lacking MRI inspections, the final study population was composed of 165 patients. The 85 patients treated between June 2016 to February 2018 were allocated to the training (cross-validation) cohort, while the rest 80 patients treated between January 2009 to December 2014 were to the testing cohort. The selected cohorts were staged by the 7th edition of the American Joint Committee on Cancer/Union for International Cancer Control TNM staging system [25]. T1-weighted (T1), contrast-enhanced T1-weighted (T1-cs), and T2-weighted (T2) MRI sequences were before and after the second cycle of NAC. All patients received NAC treatment, consisting of two to three cycles of GP regimen (gemcitabine 1000 mg/m^2/day on days 1–8, cisplatin 25 mg/m^2/day on days 1–3), TP regimen (docetaxel 60 mg/m^2/day on day 1, cisplatin 25 mg/m^2/day on days 1 to 3), and FP regimen (cisplatin25 mg/m^2/day on days 1–3, and 5-fluorouracil 500 mg/m^2/day on days 1–3) at a two-week interval before the initiation of radiotherapy.

Imaging acquisition and tumor segmentation

A 1.5 T MR scanner (Magnetom Avanto, Siemens Medical Solutions, Erlangen Germany) was utilized for the image inspection, where the reception time and echo time were 650 ms and 11 ms for T1; 940 ms and 11 ms for T1-fs; 4280 ms and 95 ms for T2, respectively. Besides, the matrix size was 256 × 224, the pixel spacing was 0.8 mm × 0.8 mm, and the slice spacing was 3.3 mm.

To evaluate the NAC early response, MR scans at two different time points were inspected, where the pre-treatment examination was at 4.32 ± 1.57 days (range 1–7 days) before NAC, and the two-cycle-end examination was at 42.77 ± 2.41 days (range 39–46 days) after the initiation of NAC. Two expert radiation oncologists delineated the primary and lymph node gross tumor volume (GTV) with MIM (MIM Software Inc., Cleveland) on the two MR inspection time-points. Dice similarity coefficient (DSC) [34,35] was computed between the two groups of segmentation to optimize the quality of delineation. As recommended by [36], we set the acceptance of the DSC threshold to be 0.7. If the segmentation had a DSC lower than 0.7, a re-delineation was implemented by discussion to guarantee the revised DSC achieve the threshold. The segmented GTV was exported in DICOM format to Matlab R2015a (The Math Works, MA, USA) for DSC computation and smoothed according to the strategy in [26] to prepare for the texture extraction process.

Criteria for NAC response

We evaluated the early response of NAC by the Response Evaluation Criteria in Solid Tumors 1.1 (RECIST 1.1) [27] and took the T1-cs sequence to assess the lesion response. NPC patients with complete response (CR) or partial response (PR) were classified into the response group. NPC patients with stable disease (SD) or progressive disease (PD) were classified into the non-response group.

Radiomics feature extraction

For all the MR sequences before NAC treatment, four shape features were extracted from the GTV region, including the volume, the longest diameter, the smallest polyhedron containing the tumor region (Solidity), and the best fitting ellipsoid (Eccentricity), respectively [24]. Besides, three first-order features and forty texture features were computed, including the skewness, kurtosis, gray-level histogram, gray-level co-occurrence matrix (GLCM), gray-level run-length matrix (GLRLM), gray-level size zone matrix (GLSZM), and neighborhood gray-tone difference matrix (NGTDM). Specifically, we applied the 3D analysis with 26 connecting voxel units for texture extraction [24]. Fig. 1 has illustrated the radiomics features extracted in this study.

To explore the potential of different extraction parameters and further improve the predictive performance, we implemented a permutation test [24] with multiple combinations of extraction parameters for the first-order and texture features concerning the weighting for wavelet band-pass filter (WW: 0.5 0.67 1.0 1.5 2.0), the isotropic voxel size (IS: pixel 1 mm 2 mm 3 mm 4 mm 5 mm), the type of quantization algorithm (QA: Equal Lloyd), and the number of gray levels for quantization (GL: 8 16 32 64). Consequently, a total of 31,920 radiomics features were extracted from GTV on the multi-sequence MR images using a toolbox developed by Vallieres [24] on MATLAB.

Feature selection

To avoid the over-fitting problem caused by relevance and redundancy, a feature reduction process was implemented in the training cohort. The stepwise forward selection scheme [24] was adopted to collectively pick up the most valuable 25 features from the large initial set after the permutation test. Specifically, with the selected i-1 number of features, the i^{th} one was to maximize

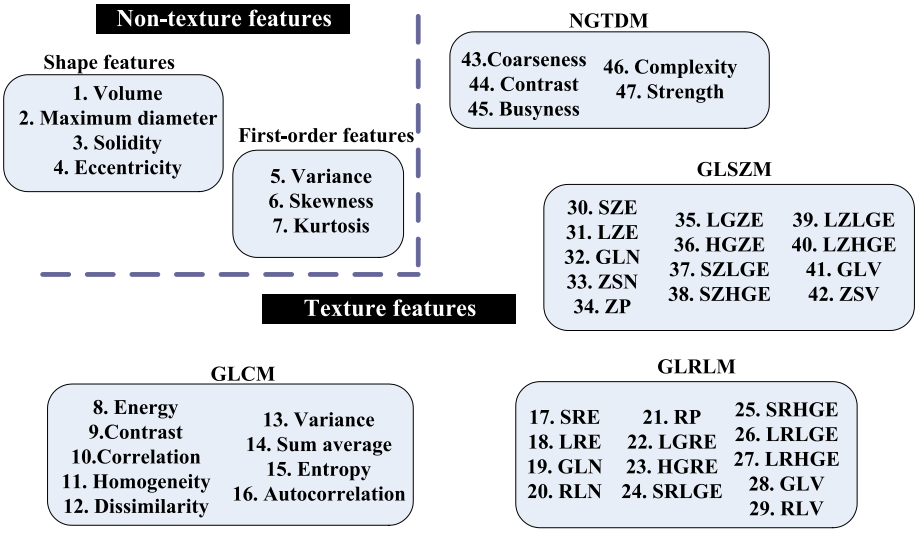

Fig. 1. Illustration for the radiomics features extracted in this study.

$$\underset{i}{argmax}[|r(x_i,y)| + \sum_{k=1}^{i-1}\frac{2(i-k)}{i(i-1)}\cdot(1-MIC(x_k,x_i))] \quad (1)$$

where y was the outcome vector of the NAC response, $r(x_i, y)$ was the Spearman's rank correlation coefficient between feature x_i and y, MIC (x_k, x_i) was the maximal information coefficient between the selected feature x_k and x_i [28]. We repeated the feature selection process 25 times and finally ranked the most valuable 25 features to build the prognosis model for NAC response.

Predictive model development

The reduced 25 features were weighted linearly as candidate predictors to build a multivariable logistic regression model in the training cohort. In this study, the linear classification model with p features was developed as

$$g(x) = c_0 + \sum_{i=1}^{p} c_i x_i \quad (2)$$

where $g(x)$ was the predicted radiomics score of the model, x_i was the i^{th}

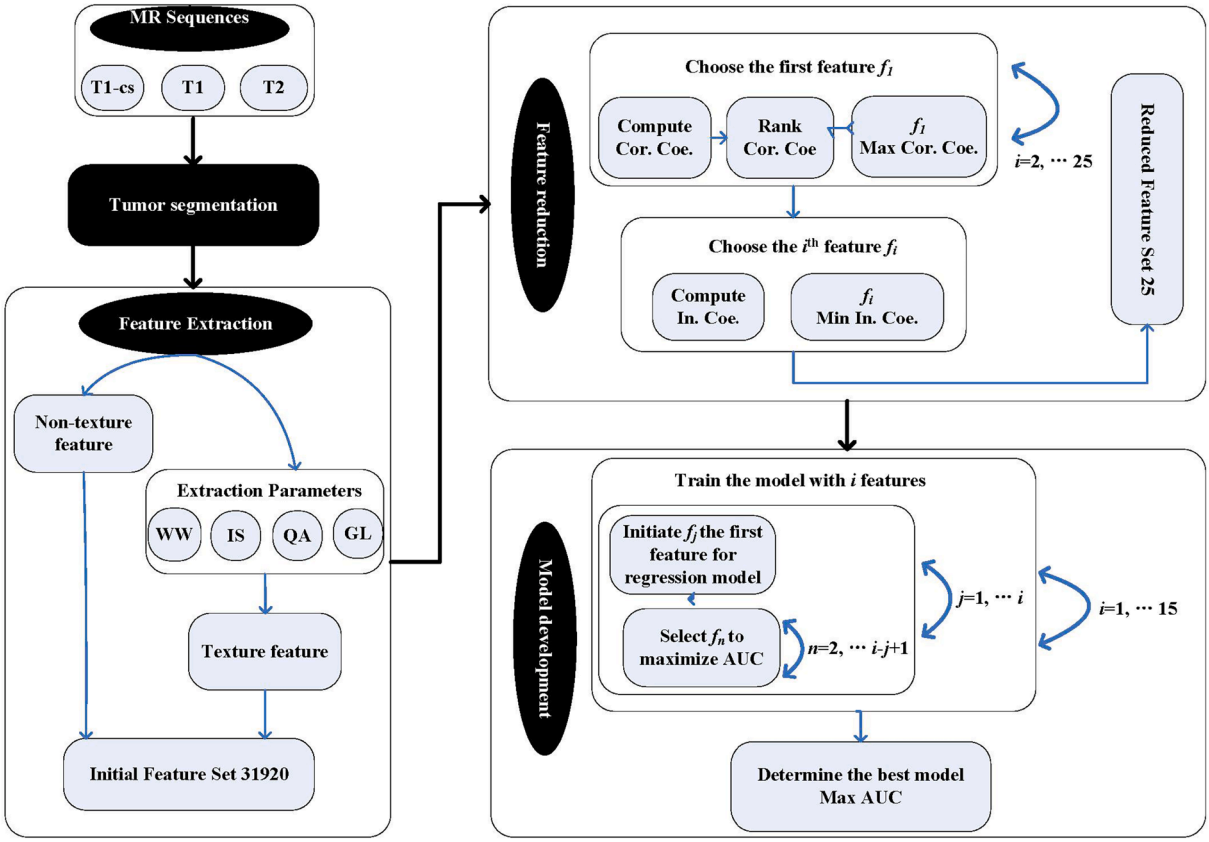

Fig. 2. Workflow of the prediction model construction process.

selected features, and c_i was the i^{th} regression coefficient. We then conducted logit transformation

$$\pi(x) = \frac{e^{g(x)}}{1 + e^{g(x)}} \quad (3)$$

to intuitively assess the NAC early response in patients with locally advanced NPC. The order of the model ranged from 1 to 10 in this study. Another stepwise forward strategy [24] was adopted to maximize the AUC estimated by bootstrapping (1000 samples). Furthermore, to increase the credibility of the prediction model, an imbalance-adjusted bootstrapping strategy [24] was applied, where the probability of a negative instance (NAC non-responder) was made equal with that of a positive instance (NAC responder). Finally, the model which provided the highest AUC was selected as the final model. Fig. 2 summarized the workflow of the model construction process.

Model validation

For the internal cross-validation, we evaluated the prediction performance by the bootstrapping (1000 samples) with AUC, sensitivity, and specificity [31] calculated. We also conducted independent testing for the 80 patients who were not involved in building the model. The corresponding AUC, sensitivity, and specificity were also computed.

Clinical application

Finally, we implemented logit transformation to the estimated radiomics scores and displayed the probable NAC early response in NPC patients straightforwardly. The probability of a positive response to NAC was calculated to help the physician with a more informed decision for individualized treatment.

Results

Clinical characteristics

In the whole cohort, 116 patients were classified into the NAC response group, while 49 were into the non-response group. Table 1 displayed the baseline characteristics of the patients. No significant differences were observed ($P > 0.1$) between the response and non-response groups to NAC.

Radiomics signature

In the training cohort, we firstly investigated the univariate association between the extracted radiomics features and the early response to NAC by the Spearman's rank correlation. Fig. 3 depicted the absolute value of the correlation coefficients, with the y-axis representing the non-texture and texture features from T1, T2, T1-cs sequences, and the x-axis representing the varied combinations of extraction parameters. Due to the space limitation, the names of the features were not completely displayed. Besides, the column side label of the heat-map was stratified into four levels, with each one representing the WW, IS, QA, GL parameters, respectively. It was observed that the texture features generally presented a higher impact on the predictive value relative to the non-texture features. Besides, the variation in extraction parameters also led to differences in the predictive value. After the dimensional reduction, 25 radiomics features were selected to build the prediction model, consisting of one from T2 and the others from T1-cs (Table 2). It could be observed that the features extracted from T1-cs presented a higher predictive value than the others.

Prediction model

Fig. 4 displayed the estimated distribution of AUC, sensitivity, and specificity by the bootstrapping (1000 samples) in the training cohort, where the model order ranged from 1 to 10. We visualized the coherent ranges of 95% confidence intervals by the error bars. Results showed that the prediction performance increased with the increasing model order when it was lower than 6. The prediction performance was optimal with model order 6. However, when it was higher than 6, the prediction performance started to decline. Therefore, we decided to choose the six features (index number as 1, 2, 6, 8, 14, 25 in Table 2) to build the final prediction model in a manner of logistic regression.

With bootstrapping (1000 samples), the average AUC, sensitivity, and specificity for cross-validation were 0.948 (95% CI: 0.944–0.951), 0.849 (95% CI: 0.845–0.853), and 0.840 (95% CI: 0.830–0.850). For the independent testing cohort, the resultant AUC, sensitivity, and

Table 1
Baseline Characteristics of NPC patient in the training-validtion and testing cohorts.

Parameters	Training and Cross-validation			Testing		
	Responder (n = 59)	Non-responder (n = 26)	*P*	Responder (n = 57)	Non-responder (n = 23)	*P*
Age (years)[b]mean ± SD	47.76 ± 12.13	45.15 ± 12.36	0.46	47.28 ± 11.42	48.00 ± 8.74	0.79
Gender [a]			0.49			0.55
Male	45 (76.27%)	18 (69.23%)		41 (71.93%)	15 (65.22%)	
Female	14 (23.72%)	8 (30.77%)		16 (28.07%)	8 (34.78%)	
Tumor stage* [a]			0.21			0.73
T1	3 (5.08%)	0		1 (1.75%)	1(4.35%)	
T2	8 (13.56%)	8 (30.77%)		17 (29.82%)	7 (30.43%)	
T3	20 (33.90%)	7 (26.92%)		18 (31.58%)	9(39.13%)	
T4	28 (47.46%)	11 (42.31%)		21 (36.84%)	6 (26.09%)	
Nodal stage* [a]			0.33			0.13
N0 (%)	1(1.69%)	1(3.85%)		0	0	
N1 (%)	2 (3.39%)	3 (11.54%)		4 (7.02%)	4 (17.39%)	
N2(%)	37 (62.71%)	12 (46.15%)		38 (66.67%)	10 (43.48%)	
N3(%)	19 (32.20%)	10 (38.46%)		15 (26.32%)	9 (39.13%)	
NAC regimen [a]			0.89			0.45
GP	19 (32.20%)	9 (34.62%)		7 (12.28%)	2 (8.70%)	
TP	21 (34.78%)	10 (38.46%)		21 (36.84%)	12 (52.17%)	
FP	19 (32.20%)	7 (26.92%)		29 (50.88%)	9 (39.13%)	
NAC period[a]			0.58			0.84
2	42 (71.19%)	20 (76.92%)		36 (63.16%)	14 (60.87%)	
3	17 (28.81%)	6 (23.08%)		21 (36.84%)	9 (39.13%)	

b Two independent sample *t* test
[a] χ^2 test
* According to the 2009 Union for International Cancer Control

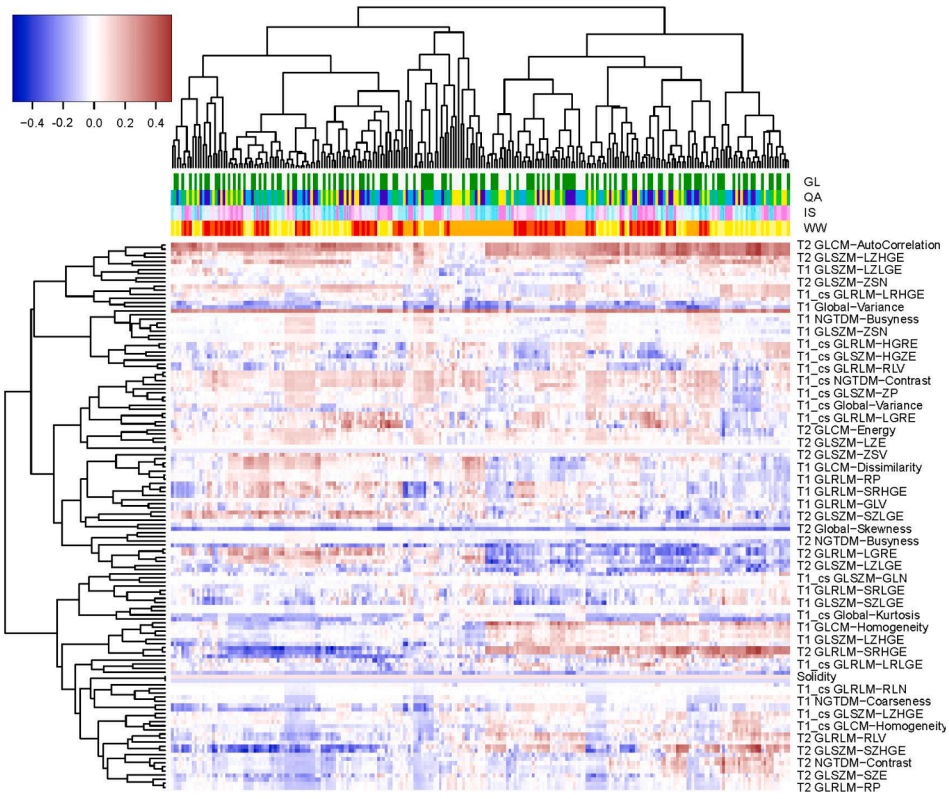

Fig. 3. Univariate association between the radiomics features and the early response of NAC in terms of the Spearman's rank correlation. The column side label is stratified into four levels with different colors representing different parameters.

Table 2
The results of the radiomics feature selection.

Index	Feature Names	Sequence	WW	IS	QA	GL
1	GLRLM-HGRE	T2	2.0	3	Equal	8
2	GLSZM-SZLGE	T1-cs	2	5		16
3	First order-Skewness		2.0	5		
4	GLCM-Contrast		0.5	4	Lloyd	
5	GLCM-Variance		1.5	3		16
6	GLCM-SumAverage		2.0	4	Equal	8
7	GLRLM-SRE		1.5	2	Lloyd	32
8	GLSZM-HGZE		2	4	Equal	8
9	GLCM-Dissimilarity		1.0			32
10	GLRLM-LRE		1.5	2	Lloyd	
11	GLCM-Homogeneity		0.67	4		8
12	GLRLM-GLN			pixel		64
13	GLRLM-RLN		1.5			
14	GLCM-Correlation		1.0	4		8
15	GLSZM-SZHGE		0.5	pixel		16
16	GLCM-Entropy		1.5	3		16
17	GLRLM-LGRE		0.5	2		32
18	GLRLM-SRLGE		1.5	5	Equal	16
19	GLRLM-SRHGE		2			32
20	GLSZM-LGZE			5	Equal	16
21	GLRLM-HGRE			5	Equal	8
22	GLCM-Energy		1.5	3	Lloyd	32
23	GLRLM-GLV			1		64
24	GLRLM-LRHGE			4		
25	GLRLM-RLV		0.67	1		32

specificity were 0.925, 0.821, and 0.792, respectively.

Clinical application

Fig. 5 (A) and (B) displayed the NAC response probability as a function of the predicted radiomics score g(x) in the cross-validation and testing cohorts. The black line denoted the result of the logit transformation π(x). The blue dots represented the response group, while the red cross represented the non-response group. For the response group, the ideal prediction result should be 1. Otherwise, it should be 0 for the non-response group. In both cohorts, very few cases yielded prediction estimates π(x) higher than 0.5 for the non-response group and lower than 0.5 for the response group. Therefore, the value 0.5 had the potential to classify the cases into the response and non-response groups. Besides, the predicted radiomics score of the response group was significantly different from that of the non-response group ($P < 0.05$) in terms of the Student's *t*-test.

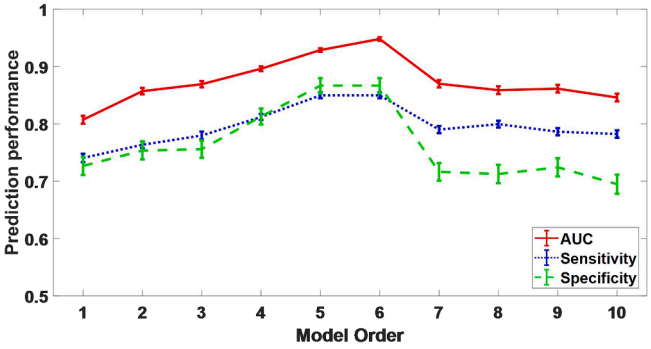

Fig. 4. Estimation of the prediction performance with model order 1–10 in the training cohort. Error bars represent the standard error of the mean on a 95% confidence interval.

Discussion

In this study, a multisequence MRI-based radiomics model was developed to individually predict the early response of NAC in advanced NPC patients before chemotherapy. The permutation of multivariable

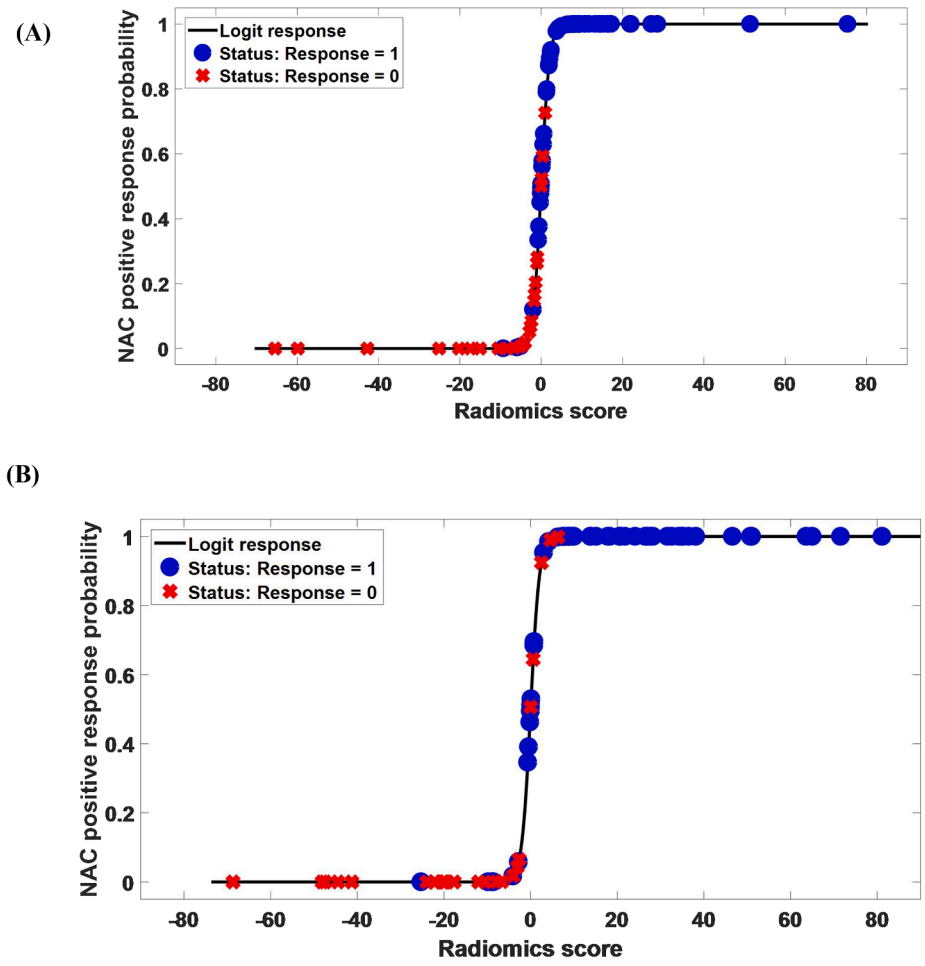

Fig. 5. NAC response probability (response = 1, non-response = 0) as a function of the predicted radiomics score. The black line displays the result of the logit transformation to the radiomics score. The blue circles represent the response group. The red crosses represent the non-response group. (A) Cross-validation cohort. (B) Testing cohort. (For interpretation of the references to colour in this figure legend, the reader is referred to the web version of this article.)

extraction parameters was implemented to improve the predictive performance. Consequently, the model, composed of 6 texture features (one from T2 and the others from T1-cs), demonstrated the optimal predictive performance. Compared with the previous studies [23], the proposed model could classify the patients into the NAC response or non-response groups with improved accuracy, indicating a promising potential to individualize the treatment for NPC patients and avoid unnecessary side effects. In addition, the estimation of NAC early response could also play an important role in the prognosis of clinical outcomes [13,29].

In this study, we observed the texture features usually had a higher correlation with the NAC early response than the non-texture features. A possible explanation was the texture features could effectively characterize the intra-tumoral heterogeneity [32,33]. In addition, the final selected features (GLRLM, GLCM) for the NAC prognosis model were in good agreement with other studies [50,51,16], given the GLCM could differentiate low-grade and high-grade lesions [51] and the GLRLM was highly associated with survival [50]. Similarly, we also found these two features important for NAC response prognosis. Furthermore, the multiple extraction parameters posed varying correlations with the NAC response. The images could produce different texture measurements with the extraction parameters, leading to a better quantitative description of the image patterns. Therefore, we deduced that the tumor heterogeneity could be better characterized by the texture features from multiple combinations of extraction parameters.

As for the prediction model, the majority of the selected features came from the T1-cs sequence, suggesting T1-cs might be better predictors among others. The high predictive potential to estimate the NAC early response in NPC patients was also demonstrated and validated. The resultant average AUCs were 0.948 (0.925), 0.849 (0.821), 0.840 (0.792) in the cross-validation and testing cohorts, respectively, which outperformed the previously published results [23,37]. A possible reason could be attributed to the contribution of the multiple combinations of extraction parameters. To our best knowledge, this study has been the first to incorporate the permutation and combination of multiple texture extraction parameters into the NAC response prognosis for NPC patients. Besides, to further improve the credibility of the prediction results, cross-validation and independent testing were implemented. Since a smaller number of non-responders than responders were noticed, we also introduced the imbalance-adjusted bootstrap strategy to decrease the statistic bias of small samples during the training process. The optimized radiomics model could predict the positive or negative response to NAC, enabling insights for risk assessment and ultimately benefiting the personalized treatment.

As has been demonstrated by several studies [9,10], NAC combined with chemoradiotherapy is very promising for improving the survival rate of advanced NPC patients. The effort to connect radiomics with PFS (progression-free survival) and OS (overall survival) should be highly recognized since the improvement for PFS and OS is the ultimate goal for cancer treatment. However, as the first stage of treatment, not all patients responded well to NAC. The identification of non-responders should also be important. Otherwise, unnecessary toxicity and overtreatment could be suffered, deteriorating the PFS and OS with high probability. Therefore, this study mainly focused on the prognosis for the NAC-only response. Besides, such a prognosis could also help with

clinical treatment. For instance, the identification of a non-responder might suggest an effort to try alternative therapy combinations to improve clinical outcomes. The prognosis of NAC long-term response requires further investigation.

Historically, the tumor node metastases (TNM) staging system has served as the major prognostic factor in predicting therapeutic outcomes for NPC [39,40]. Although this approach provides frameworks for outcome prediction, they are limited by tumor heterogeneity within stage categories, hampering accurate prognosis for individual patients [41]. According to [37], The training and validation AUC were only 0.708 and 0.549 by the clinical prognosis model. Besides, anatomical MRI has also been widely used to determine the treatment response in NPC [42]. For diffusion-weighted (DW) MRI, several studies have validated that apparent diffusion coefficient (ADCs) could be a valuable biomarker to predict the response of NAC [43,44]. However, the findings regarding ADCs might sometimes be confounding. It is demonstrated that low pretreatment ADCs tend for a better response to NAC [44]. However, High ADC values or large ADC increase after the initiation of NAC could also indicate a better chemoradiotherapy response [43]. The accurate association between ADCs and NAC response remains for investigation. In addition, the Plasma Epstein Barr virus (EBV) DNA level has also been widely accepted as a valuable biomarker for NPC prognosis. Its predictive potential is successfully validated for recurrence, metastasis, and survival of NPC patients [45–47]. The chronic inflammation induced by EBV could also be significant for progression and aggressiveness in NPV patients [48]. A recent study has also shown the complement of NAC before CCRT could reduce distant failure in NPC patients with stage N0-1 disease and EBV DNA lower than 4,000 copies/mL [49]. However, the correlation between EBV DNA level and NAC response of NPC patients remains to be recognized.

This study has several limitations that need to be acknowledged. First, although the NAC early response was assessed at the end of the second cycle for each patient, we did not control the regimen and treatment cycles constant, probably influencing the predictive potential and introducing confounds for result interpretation. Since different physicians might have their personal preference for the regimen and deciding the exact number of cycles before treatment is difficult, there could be a considerable decrease in the study population if these two variables were controlled. The other studies also face this problem [37,43], and an increase in the number of enrolled patients could be a solution. In addition, although the baseline characteristics between training and testing cohorts were not significantly different in Table 1, there might still be potential selection bias due to the single-center nature of the study. To address it, external testing in terms of multi-institutional cohorts, collected from collaborating institutions or cancer imaging archive (TCIA) [38], remains to be explored in our future studies. However, the variable control for multicentral study should also be specially paid attention to. For example, the NAC regimen in Europe, commonly recommended as the TPF combination [52], could be different from that in China. Finally, since radiomics has demonstrated a significant correlation with tumor pathology, combining molecular and genetic biomarkers with the current prognosis model could be an attractive extension. The association between radiomics and molecular genetic biology in NAC prognosis demands further investigation.

Conclusion

In this study, an MRI-based radiomics model was developed and demonstrated promising capability for the individual prediction of NAC response in NPC patients. In particular, we have optimized the multiple combinations of texture extraction parameters by permutation test and observed an improved prediction performance relative to the previously published works. The proposed prediction model could help the radiation oncologist to a more informed decision for the NAC individualized treatment while retrenching the cost of clinical resources simultaneously.

Declaration of Competing Interest

The authors declare that they have no known competing financial interests or personal relationships that could have appeared to influence the work reported in this paper.

Acknowledgements

This work was supported by the Natural Science Foundation of China (NSFC) under Grant 61901087, Chengdu Science and Technology Program under Grant 2019-YF05-00022-SN.

References

[1] Tang L-L, Chen W-Q, Xue W-Q, He Y-Q, Zheng R-S, Zeng Y-X, et al. Global trends in incidence and mortality of nasopharyngeal carcinoma. Cancer Lett 2016;374(1):22–30.
[2] Bray F, Ferlay J, Soerjomataram I, Siegel RL, Torre LA, Jemal A. Global cancer statistics 2018: GLOBOCAN estimates of incidence and mortality worldwide for 36 cancers in 185 countries. CA Cancer J Clin 2018;68(6):394–424.
[3] Chen L, Mao Y-P, Xie F-Y, Liu L-Z, Sun Y, Tian Li, et al. The seventh edition of the UICC/AJCC staging system for nasopharyngeal carcinoma is prognostically useful for patients treated with intensity-modulated radiotherapy from an endemic area in China. Radiother Oncol 2012;104(3):331–7.
[4] Al-Sarraf M, LeBlanc M, Giri PG, Fu KK, Cooper J, Vuong T, et al. Chemoradiotherapy versus radiotherapy in patients with advanced nasopharyngeal cancer: phase III randomized Intergroup study 0099. J Clin Oncol 1998;16(4):1310–7.
[5] Lee AWM, Tung SY, Chua DTT, Ngan RKC, Chappell R, Tung R, et al. Randomized trial of radiotherapy plus concurrent-adjuvant chemotherapy vs radiotherapy alone for regionally advanced nasopharyngeal carcinoma. J Natl Cancer Inst 2010;102(15):1188–98.
[6] Baujat B, Audry H, Bourhis J, Chan ATC, Onat H, Chua DTT, et al. Chemotherapy in locally advanced nasopharyngeal carcinoma: an individual patient data meta-analysis of eight randomized trials and 1753 patients. Int J Radiat Oncol Biol Phys 2006;64(1):47–56.
[7] OuYang PY, Xie C, Mao YP, Zhang Y, Liang XX, Su Z, et al. Significant efficacies of neoadjuvant and adjuvant chemotherapy for nasopharyngeal carcinoma by meta-analysis of published literature-based randomized, controlled trials. Ann Oncol 2013;24(8):2136–46.
[8] Chen Y-P, Guo R, Liu Na, Liu Xu, Mao Y-P, Tang L-L, et al. Efficacy of the Additional Neoadjuvant Chemotherapy to Concurrent Chemoradiotherapy for Patients with Locoregionally Advanced Nasopharyngeal Carcinoma: a Bayesian Network Meta-analysis of Randomized Controlled Trials. J Cancer 2015;6(9):883–92.
[9] Wang M, Tian H, Li G, Ge T, Liu Y, Cui J, et al. Significant benefits of adding neoadjuvant chemotherapy before concurrent chemoradiotherapy for locoregionally advanced nasopharyngeal carcinoma: a meta-analysis of randomized controlled trials. Oncotarget 2016;7(30):48375–90.
[10] Wang F, Jiang C, Wang L, Yan F, Sun Q, Ye Z, et al. Influence of concurrent chemotherapy on locoregionally advanced nasopharyngeal carcinoma treated with neoadjuvant chemotherapy plus intensity-modulated radiotherapy: a retrospective matched analysis. Sci Rep. 2020;10(1):2489.
[11] Hui EP, Ma BB, Leung SF, King AD, Mo F, Kam MK, et al. Randomized phase II trial of concurrent cisplatin-radiotherapy with or without neoadjuvant docetaxel and cisplatin in advanced nasopharyngeal carcinoma. J Clin Oncol 2009;27(2):242–9.
[12] Fountzilas G, Ciuleanu E, Bobos M, Kalogera-Fountzila A, Eleftheraki AG, Karayannopoulou G, et al. Induction chemotherapy followed by concomitant radiotherapy and weekly cisplatin versus the same concomitant chemoradiotherapy in patients with nasopharyngeal carcinoma: a randomized phase II study conducted by the Hellenic Cooperative Oncology Group (HeCOG) with biomarker evaluation. Ann Oncol 2012;23(2):427–35.
[13] Peng H, Chen L, Zhang Y, Li W-F, Mao Y-P, Liu Xu, et al. The Tumour Response to Induction Chemotherapy has Prognostic Value for Long-Term Survival Outcomes after Intensity-Modulated Radiation Therapy in Nasopharyngeal Carcinoma. Sci Rep 2016;6(1). https://doi.org/10.1038/srep24835.
[14] Schmidt MA, Payne GS. Radiotherapy planning using MRI. Phys Med Biol 2015;60(22):R323–61.
[15] Gurney-Champion OJ, McQuaid D, Dunlop A, Wong KH, Welsh LC, Riddell AM, et al. MRI-based Assessment of 3D intrafractional motion of head and neck cancer for radiation therapy. Int J Radiat Oncol Biol Phys. 2018;100(2):306–16.
[16] Aerts HJWL, Velazquez ER, Leijenaar RTH, Parmar C, Grossmann P, Carvalho S, et al. Decoding tumour phenotype by noninvasive imaging using a quantitative radiomics approach. Nat Commun. 2014;5(1):4006.
[17] Gillies RJ, Kinahan PE, Hricak H. Radiomics: images are more than pictures, they are data. Radiology. 2016;278(2):563–77.
[18] Lambin P, Rios-Velazquez E, Leijenaar R, Carvalho S, van Stiphout RGPM, Granton P, et al. Radiomics: extracting more information from medical images using advanced feature analysis. Eur J Cancer. 2012;48(4):441–6.
[19] Zhang B, He X, Ouyang F, Gu D, Dong Y, Zhang Lu, et al. Radiomic machine-learning classifiers for prognostic biomarkers of advanced nasopharyngeal carcinoma. Cancer Lett. 2017;403:21–7.

[20] Zhuo E-H, Zhang W-J, Li H-J, Zhang G-Y, Jing B-Z, Zhou J, et al. Radiomics on multi-modalities MR sequences can subtype patients with non-metastatic nasopharyngeal carcinoma (NPC) into distinct survival subgroups. Eur Radiol. 2019;29(10):5590–9.
[21] Zhang Lu, Zhou H, Gu D, Tian J, Zhang B, Dong Di, et al. Radiomic nomogram: pretreatment evaluation of local recurrence in nasopharyngeal carcinoma based on MR Imaging. J Cancer. 2019;10(18):4217–25.
[22] Liu J, Mao Yu, Li Z, Zhang D, Zhang Z, Hao S, et al. Use of texture analysis based on contrast-enhanced MRI to predict treatment response to chemoradiotherapy in nasopharyngeal carcinoma. J Magn Reson Imaging. 2016;44(2):445–55.
[23] Wang G, He L, Yuan C, Huang Y, Liu Z, Liang C. Pretreatment MR imaging radiomics signatures for response prediction to induction chemotherapy in patients with nasopharyngeal carcinoma. Eur J Radiol. 2018;98:100–6.
[24] Vallières M, Freeman CR, Skamene SR, El Naqa I. A radiomics model from joint FDG-PET and MRI texture features for the prediction of lung metastases in soft-tissue sarcomas of the extremities. Phys Med Biol. 2015;60(14):5471–96.
[25] A. Edge SB, D.R. Compton, C.C. Fritz, A.G. Greene, F.L. Trotti. AJCC Cancer Staging Manual, 7th edition: Springer; 2009.
[26] Deasy JO, Blanco AI, Clark VH. CERR: a computational environment for radiotherapy research. Med Phys. 2003;30(5):979–85.
[27] Eisenhauer EA, Therasse P, Bogaerts J, Schwartz LH, Sargent D, Ford R, et al. New response evaluation criteria in solid tumours: revised RECIST guideline (version 1.1). Eur J Cancer. 2009;45(2):228–47.
[28] Reshef DN, Reshef YA, Finucane HK, Grossman SR, McVean G, Turnbaugh PJ, et al. Detecting Novel Associations in Large Data Sets. 2011;334(6062):1518-24.
[29] Liu L-T, Tang L-Q, Chen Q-Y, Zhang Lu, Guo S-S, Guo L, et al. The Prognostic Value of Plasma Epstein-Barr Viral DNA and tumor response to neoadjuvant chemotherapy in advanced-stage nasopharyngeal carcinoma. Int J Radiat Oncol Biol Phys. 2015;93(4):862–9.
[30] Lambin P, Leijenaar RTH, Deist TM, Peerlings J, de Jong EEC, van Timmeren J, et al. Radiomics: the bridge between medical imaging and personalized medicine. Nat Rev Clin Oncol. 2017;14(12):749–62.
[31] Fehr D, Veeraraghavan H, Wibmer A, Gondo T, Matsumoto K, Vargas HA, et al. Automatic classification of prostate cancer Gleason scores from multiparametric magnetic resonance images. Proc Natl Acad Sci U S A. 2015;112(46):E6265–73.
[32] El Naqa I, Grigsby PW, Apte A, Kidd E, Donnelly E, Khullar D, et al. Exploring feature-based approaches in PET images for predicting cancer treatment outcomes. Pattern Recognit. 2009;42(6):1162–71.
[33] Cook GJR, Yip C, Siddique M, Goh V, Chicklore S, Roy A, et al. Are pretreatment 18F-FDG PET tumor textural features in non-small cell lung cancer associated with response and survival after chemoradiotherapy. J Nucl Med 2013;54(1):19–26.
[34] Dice LR. Measures of the amount of ecologic association between species. Ecology 1945;26:297–302.
[35] Fleiss JL. The measurement of interrater agreement. In: Statistical methods for rates and proportions. 2nd ed. New York, NY: John Wiley & Sons; 1981. p. 212–36.
[36] Zijdenbos AP, Dawant BM, Margolin RA, Palmer AC. Morphometric analysis of white matter lesions in MR images: method and validation. IEEE Trans Med Imaging. 1994;13(4):716–24.
[37] Zhao L, Gong J, Xi Y, Xu M, Li C, Kang X, et al. MRI-based radiomics nomogram may predict the response to induction chemotherapy and survival in locally advanced nasopharyngeal carcinoma. Eur Radiol 2020;30(1):537–46.
[38] Clark K, Vendt B, Smith K, Freymann J, Kirby J, Koppel P, et al. The Cancer Imaging Archive (TCIA): maintaining and operating a public information repository. J Digit Imaging 2013;26(6):1045–57.
[39] Cadoni G, Giraldi L, Petrelli L, Pandolfini M, Giuliani M, Paludetti G, et al. Prognostic factors in head and neck cancer: a 10-year retrospective analysis in a single-institution in ItalyFattori prognostici del tumore testa-collo: unanalisi retrospettiva monocentrica di 10 anni. Acta Otorhinolaryngol Ital. 2017;37(6):458–66.
[40] Zaravinos A. An updated overview of HPV-associated head and neck carcinomas. Oncotarget. 2014;5(12):3956–69.
[41] Garden AS, Asper JA, Morrison WH, Schechter NR, Glisson BS, Kies MS, et al. Is concurrent chemoradiation the treatment of choice for all patients with Stage III or IV head and neck carcinoma? Cancer 2004;100(6):1171–8.
[42] Liao X-B, Mao Y-P, Liu L-Z, Tang L-L, Sun Y, Wang Y, et al. How does magnetic resonance imaging influence staging according to AJCC staging system for nasopharyngeal carcinoma compared with computed tomography? Int J Radiat Oncol Biol Phys. 2008;72(5):1368–77.
[43] Chen YunBin, Liu X, Zheng D, Xu L, Hong L, Xu Y, et al. Diffusion-weighted magnetic resonance imaging for early response assessment of chemoradiotherapy in patients with nasopharyngeal carcinoma. Magn Reson Imaging. 2014;32(6):630–7.
[44] Zhang G-Y, Wang Y-J, Liu J-P, Zhou X-H, Xu Z-F, Chen X-P, et al. Pretreatment Diffusion-Weighted MRI can predict the response to neoadjuvant chemotherapy in patients with nasopharyngeal carcinoma. Biomed Res Int 2015;2015:1–8.
[45] Chua MLK, Wee JTS, Hui EP, Chan ATC. Nasopharyngeal carcinoma. Lancet 2016;387(10022):1012–24.
[46] Peng H, Li Z, Long Y, Li J, Liu Z, Zhou R. Clinical value of a plasma Epstein-Barr virus DNA assay in the diagnosis of recurrent or metastatic nasopharyngeal carcinoma: a meta-analysis. Biosci Rep 2019;39(9).
[47] Qiu W, Lv X, Guo X, Yuan Y. Clinical Implications of Plasma Epstein-Barr Virus DNA in children and adolescent nasopharyngeal carcinoma patients receiving intensity-modulated radiotherapy. Front Oncol. 2020;10:356.
[48] Elgui de Oliveira D, Müller-Coan BG, Pagano JS. Viral carcinogenesis beyond malignant transformation: EBV in the progression of human cancers. Trends Microbiol 2016;24(8):649–64.
[49] Liu L-T, Chen Q-Y, Tang L-Q, Guo S-S, Guo L, Mo H-Y, et al. Neoadjuvant or Adjuvant Chemotherapy Plus Concurrent CRT Versus Concurrent CRT Alone in the Treatment of Nasopharyngeal Carcinoma: A Study Based on EBV DNA. J Natl Comprehensive Cancer Network: JNCCN. 2019;17(6):703–10.
[50] Zhai T-T, van Dijk LV, Huang B-T, Lin Z-X, Ribeiro CO, Brouwer CL, et al. Improving the prediction of overall survival for head and neck cancer patients using image biomarkers in combination with clinical parameters. Radiother Oncol. 2017;124(2):256–62.
[51] Sanduleanu S, Woodruff HC, de Jong EEC, van Timmeren JE, Jochems A, Dubois L, et al. Tracking tumor biology with radiomics: a systematic review utilizing a radiomics quality score. Radiother Oncol. 2018;127(3):349–60.
[52] Ferrari D, Ghi MG, Franzese C, Codeca C, Gau M, Fayette J. The slippery role of induction chemotherapy in head and neck cancer: myth and reality. Front Oncol 2020;10:7.